

Numerical methods are used to examine the process of formation and development of a laser radiation absorption wave in a solid medium. Radiation propagation within the material is described in the geometric optics approximation.

Thermal ejection of electrons from the valent zone into the conduction band of a solid medium under the action of laser radiation leads to the development of thermal avalanche breakdown. As a result, within the initially transparent dielectric an opaque zone is formed, and an absorption wave which absorbs the incident radiation develops.

A laser thermal breakdown mechanism has been proposed to explain experiments with brief laser pulses, but direct experimental proof of the existence of this mechanism has been obtained for millisecond pulses acting on silicate glasses [1, 2].

The main parameters of the absorption wave are its velocity  $v$  and the temperature behind the absorption front  $T_{\max}$ ; also of interest is the width of the absorption wave front. In [3-5] analytical expressions were obtained for  $v$  and  $T_{\max}$  as functions of the material parameters (forbidden zone width  $E_g$ , electron collision frequency, phonon thermal conductivity coefficient, etc.) and the incident radiation intensity. The numerical computation of [6] obtained profiles of temperature and incident radiation intensity on the wave front and the dependences of front width and velocity of stationary absorption wave motion on incident radiation intensity for fused quartz.

All these theoretical studies considered the steady state one-dimensional motion of an absorption wave in the final stage of thermal instability development, independent of the cause of the instability - local absorbing inhomogeneities or heating of the matrix. Moreover, the above studies assumed that the thermal conductivity of the dielectric had a negligible temperature dependence, so that heat transfer was completely determined by the phonon mechanism. In fact, even at temperatures of  $\sim 4000^\circ\text{C}$  the electron thermal conductivity of glass is comparable to the phonon component, while at temperatures of  $\sim 8000^\circ\text{C}$  the electron component is the dominant one.

In connection with this, it is of interest to study an absorption wave within the volume of a solid medium with consideration of electronic thermal conductivity, and also to study the dynamics of absorption wave development over time and the effect of experimental geometry on absorption wave characteristics. For this purpose a numerical solution was sought to describe the nonsteady-state motion of an absorption wave with consideration of electronic thermal conductivity.

**Fundamental Equations.** The fundamental equations of the problem are the thermal conductivity equation with temperature dependent thermal conductivity coefficient and heat source function, and the equation for the radiation field. Since, as was shown by preliminary calculations, the width of the absorption wave front is greater than the wavelength of the incident radiation ( $\lambda = 1.06 \mu\text{m}$ ), we may use the geometric optics approximation. The system of equations then takes on the form

$$\frac{\partial T}{\partial t} = \text{div} \left( \frac{\kappa(T)}{C} \nabla T \right) + \frac{k(T)}{C} q, \quad \frac{dq}{dx} = k(T) q. \quad (1)$$

In correspondence with the semiconductor model, the temperature dependence of the absorption coefficient can be represented as

$$k(T) = k_l + k_0 \exp(-E_g/2T), \quad (2)$$

where  $E_g$  is the forbidden zone width, defined for media with unordered structures as the energy gap between the edges of valent zone mobility and the conduction zone;  $k_l$  is the linear absorption coefficient, determined,

for example, by impurities and defects, and is assumed temperature independent. For the majority of semiconductors we have  $E_g(T) = E_g(0) - \gamma T$ , where  $\gamma$  is a constant of the material, and consideration of the temperature dependence of  $E_g$  in the case  $E_g(T) > hc/\lambda$  leads only to a reevaluation of the constant  $k_0$ .

The thermal conductivity coefficient, with consideration of both phonon and electron mechanisms, has the form

$$\kappa(T) = \kappa_p + \kappa_e T \exp(-E_g/2T). \quad (3)$$

The electronic thermal conductivity can be determined from the dc conductivity using the Wiedemann-Franz formula. For solids [7], the conductivity due to free electrons obeys the law  $\sigma(T) = \sigma_0 \exp(-E_g/2T)$ , whence follows Eq. (3).

System (1) was solved for both one- and two-dimensional cases. (The solutions of the two-dimensional problem are sufficient for consideration of actual experimental geometry [2], since the lens system usually forms an axisymmetric radiation flux within the material with a caustic whose length is 7-10 times that of the focus spot.)

The initial and boundary conditions have the form

$$T(x, 0) = \frac{T_{in}}{1 + x^2/L^2}, \quad q(x_{bound}) = q_0 \quad (4)$$

for the one-dimensional problem and

$$T(x, r, 0) = \frac{T_{in} \exp(-r^2/a^2)}{1 + x^2/L^2}, \quad q(x_{bound}) = q_0 \exp(-r^2/a^2) \quad (5)$$

for the two-dimensional case.

For the numerical calculations, the following values were chosen for the constants entering into the equations and initial and boundary conditions (ZhS12 silicate glass):  $C = 3.1 \text{ J/cm}^3 \cdot \text{K}$ ;  $E_g = 3.8 \text{ eV} = 44,000 \text{ K}$  [2];  $k_l = 0.25 \text{ cm}^{-1}$ ;  $\kappa_p = 1.5 \cdot 10^{-2} \text{ W/cm} \cdot \text{K}$ ;  $T_{in} = 2500 \text{ K}$ ;  $L = 0.12 \text{ cm}$ ;  $a = 0.02 \text{ cm}$ ;  $x_{bound} = 0.15 \text{ cm}$ .

Calculations were performed for various values of incident radiation power density  $q_0$  over the range  $10^5 - 3 \cdot 10^7 \text{ W/cm}^2$ . In addition,  $k_0$  values were varied from  $2.5 \cdot 10^4$  to  $10^5 \text{ cm}^{-1}$  and  $\kappa_e$  from  $2.9 \cdot 10^{-4}$  to  $2.9 \cdot 10^{-3} \text{ W/cm} \cdot \text{deg}^2$ .

**Main Results.** Temperature profiles were calculated for various durations of laser action at several values of the parameters  $q_0$ ,  $k_0$ ,  $\kappa_e$ . The calculations revealed that steady-state motion of a two-dimensional absorption wave along the  $x$  axis occurs with the same velocity and the absorption front has the same maximum temperature as in the one-dimensional case. This is true because on the axis the radius of curvature ( $R_{curv} \gtrsim 10^{-2} \text{ cm}$ ) of the absorption wave front greatly exceeds the thickness of the front ( $d_{fr} \sim 5 \cdot 10^{-4} \text{ cm}$ ). At the same time, because of two-dimensional diffusion, the temperature profiles behind the front differ significantly.

Figure 1 shows isotherms of the absorption wave for various times for an incident radiation intensity  $q_0 = 10^6 \text{ W/cm}^2$ . A typical pattern of the change in temperature profiles with time is shown for the one-dimensional case in Fig. 2.

Since the main parameters of the absorption wave front ( $T_{max}$  and  $v$ ) coincide for the one- and two-dimensional cases, development of the wave can be studied in the one-dimensional case.

One can clearly see three stages in the development of thermal instability. In the first stage there is a sharp decrease in radiation absorption length  $l_a$ , with a related asymmetric increase in temperature profile. Up to the beginning of this stage at  $T \lesssim 2500 \text{ K}$  the length  $l_a$  is of the order of or greater than the focal length, and specimen heating due to radiation absorption occurs practically symmetrically with respect to the center of the caustic. At the end of this stage the temperature reaches a value of  $3000 - 4500 \text{ K}$ ,  $l_a \sim (0.1 - 0.01)L$ , and the temperature profile is significantly asymmetric. The maximum of the temperature profile shifts toward the incident radiation, and the speed of this shift increases with passage of time.

In the second stage there is a further increase in the steepness of the asymmetric temperature profile, and a nonsteady-state absorption wave is formed. The maximum temperature then increases, and in accordance with the expression [8]

$$Cv(T_{max} - T_{in}) = q_0 \quad (6)$$

the velocity of temperature profile front motion falls. Equation (6) is applicable in the second stage because the incident radiation is absorbed mainly in the front of the wave. The width of the absorption wave front in the

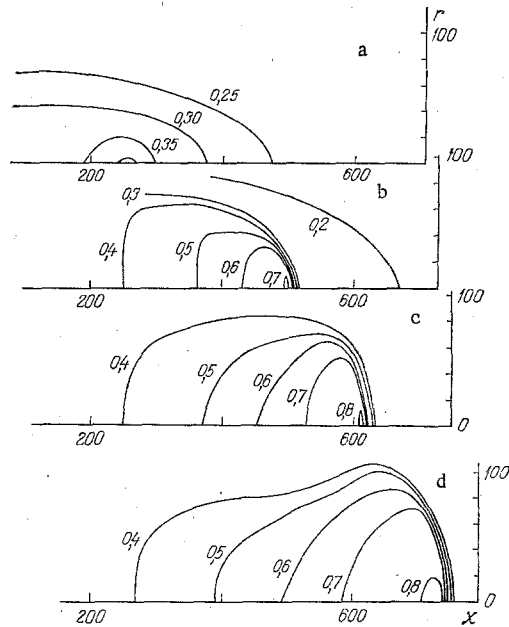


Fig. 1. Absorption wave isotherm structure for various times ( $k_0 = 5 \cdot 10^4 \text{ cm}^{-1}$ ;  $\kappa_e = 2.9 \cdot 10^{-4} \text{ W/cm} \cdot \text{deg}^2$ ; numbers along curves denote temperature in  $10^4 \text{ K}$ ); a)  $t = 256$ ; b) 512; c) 768; d)  $1024 \mu\text{sec}$ .  $r, x, \mu\text{m}$ .

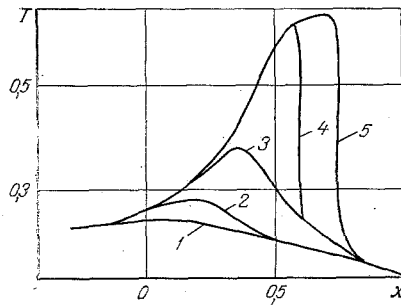


Fig. 2

Fig. 2. Temperature profiles for one-dimensional case ( $q_0 = 10^6 \text{ W/cm}^2$ ;  $\kappa_e = 1.45 \cdot 10^{-3} \text{ W/cm} \cdot \text{deg}^2$ ;  $k_0 = 10^5 \text{ cm}^{-1}$ ); 1-5) times 0, 100, 200, 400, 600  $\mu\text{sec}$ , respectively.  $T, 10^4 \text{ K}$ ;  $x, \text{mm}$ .

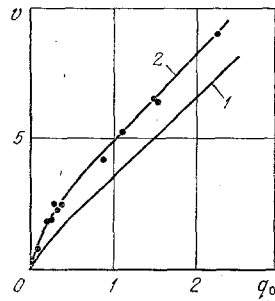


Fig. 3

Fig. 3. Velocity of steady-state absorption wave motion versus incident radiation intensity: 1,  $k_0 = 5 \cdot 10^4 \text{ cm}^{-1}$ ;  $\kappa_e = 2.9 \cdot 10^{-4} \text{ W/cm} \cdot \text{deg}^2$ ; 2)  $10^5$  and  $1.45 \cdot 10^{-3}$ ; points, experiment [2].  $v, \text{m/sec}$ ;  $q_0, 10^7 \text{ W/cm}^2$ .

course of the second stage decreases significantly (from several hundred  $\mu\text{m}$  to several  $\mu\text{m}$  at the end).

In the third stage of thermal instability development the temperature and velocity achieve a steady-state regime and a purely thermal conductivity regime of absorption wave propagation is realized.

The velocity of the steady-state absorption wave motion is shown as a function of incident radiation intensity for various values of the coefficients  $\kappa_e$  and  $k_0$  in Fig. 3. Also shown are experimental points for ZhS12 glass [2]. The experimental data are described best by the values  $k_0 = 10^5 \text{ cm}^{-1}$ ,  $\kappa_e = 1.45 \cdot 10^{-3} \text{ W/cm} \cdot \text{deg}^2$ .

We note that because of improper consideration of the geometric factor (nonrectangular temperature profile) in [2], the value of the preexponential factor for ZhS12 glass is an order of magnitude too low. (We are indebted to D. B. Chopornyak for calling this fact to our attention.) Due to experimental uncertainty the electrical

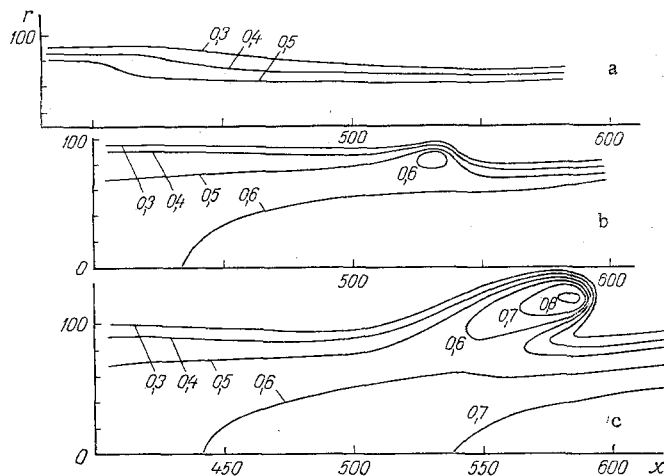


Fig. 4. Satellite absorption wave at  $q_0 = 3.2 \cdot 10^6$  W/cm<sup>2</sup>; a)  $t = 256$ ; b) 342; c) 432  $\mu$ sec.

conductivity was determined to within a factor of two, and within the limits of this uncertainty the value of  $\kappa_e$  and the experimental  $\sigma$  quantitatively satisfy the Wiedemann-Franz law. The time required to establish the steady-state regime depends significantly on the intensity of the incident radiation. This dependence is approximated well by a power function, and at the values  $k_0 = 5 \cdot 10^4$  cm<sup>-1</sup>,  $\kappa_e = 2.9 \cdot 10^{-4}$  W/cm<sup>2</sup>·deg<sup>2</sup> has the form  $t = 1.4 \cdot 10^2 q_0^{-0.9}$ , where  $q_0$  is measured in W/cm<sup>2</sup> and  $t$  in sec. Calculations show that increase in the absorption coefficient changes the parameters of the absorption wave insignificantly. Thus, increase in  $k_0$  by a factor of two leads to an increase in velocity and decrease in temperature by less than 10% for  $q_0 = 10^6$  W/cm<sup>2</sup>; at  $q_0 = 10^7$  W/cm<sup>2</sup> the corresponding changes in the absorption wave parameters are about 15%. Variation of  $E_g$  by 20% changes the wave velocity by 6%. The dependence of the absorption wave parameters on the value of the electronic thermal conductivity coefficient is also quite weak. Thus, for an increase in  $\kappa_e$  by an order of magnitude, the absorption wave velocity increases by 37%, while the time for establishment of the steady-state regime and maximum temperature in the absorption wave decrease by 20%. A more marked dependence upon  $\kappa_e$  is shown by the absorption front width  $d_{fr}$ , which is defined as the distance in which the laser radiation intensity changes from 0.9 to 0.1  $q_0$ . With increase in  $\kappa_e$  by an order of magnitude,  $d_{fr}$  increases by a factor of approximately two.

**"Satellite" Absorption Wave.** At some ratio of the medium's parameters (see below) during the process of absorption wave development there appears a unique "satellite" absorption wave on the periphery of the optical discharge. It begins to form from a projection on the isotherm  $(0.3-0.4) \cdot 10^4$ °K (Fig. 4a). The absorption length produced by the reverse breaking effect at a temperature of  $0.3 \cdot 10^4$ °K,  $l_a \sim 100$   $\mu$ m, and at  $0.4 \cdot 10^4$ °K,  $l_a \sim 10$   $\mu$ m, i.e., as is evident from Fig. 4a, the laser radiation penetrates to the projection on the  $0.4 \cdot 10^4$ °K isotherm and is totally absorbed there. As a result, the front of the projection becomes sharper and a detached absorption wave develops (Fig. 4b, c). To form this projection, a change in the form of the isotherms during absorption wave motion is necessary.

In the initial stage of the motion the temperature field has isotherms close in form to paraboloids of revolution (see Fig. 1a, b), while the final form of the isotherms in the last stage is close to pear-shaped (Fig. 1c, d). There also exists a time in the process when in the interval  $(x_1, x_2)$  the values of the isotherm  $x$ -coordinates have a cylindrical form. The temperature field at  $x < x_1$  (where the isotherms are part of a paraboloid) forms a projection, and the portion of the temperature field at  $x > x_2$ , expanding over coordinate  $r$  during motion, encourages effective "repulsion" of the satellite wave formed. The latter can be seen clearly by comparing Fig. 4b and c. In order that the developing projection not disappear due to thermal diffusion and that the satellite wave form itself before the expansion of the main part of the discharge, it is necessary that certain relationships exist between the intensity-dependent absorption and thermal conductivity coefficients. The range of material parameters over which the peripheral wave would be observed at various intensities was not determined; we note only that this effect is observed at  $q_0 = 3.2 \cdot 10^6$  W/cm<sup>2</sup>, at  $k_0 = 5 \cdot 10^4$  cm<sup>-1</sup>, and  $\kappa_e = 2.9 \cdot 10^{-4}$  W/cm<sup>2</sup>·deg<sup>2</sup>. When these parameters are increased or decreased by a factor of two, the peripheral wave does not develop. Modulation of the laser radiation ( $\sim 30-40\%$ ) leads to formation of several satellite waves on the periphery of the optical discharge.

The main peculiarities of absorption wave development in glass are described well by the semiconductor model even though the model is not completely adequate. Thus, thermal dissipation of the medium [9] was not

considered in the calculations, nor was thermal expansion of the discharge region and surrounding liquid glass volume, nor the dependence of electron collision frequency, heat capacity, and ionization potential upon temperature.

The theoretical and experimental dependences of velocity on intensity show good qualitative agreement, and there is satisfactory agreement (with consideration of expansion) between the values of absorption wave velocity.

The location of the most strongly heated region (with  $T > 4 \cdot 10^3 \text{K}$ ) at the caustic of the focusing lens also agrees with experimental data. In the process of thermal instability development the further (with respect to the incident radiation) boundary of this region is located at some distance from the caustic in the direction toward the lens, and remains practically unchanged with time [10].

The two-dimensional absorption wave calculated has a form close to a paraboloid of revolution in the initial stage of steady-state motion (which agrees with the experiments of [1]) but changes to a pear-shaped form as motion continues. Such a transition has not been observed in experiment, and so the fine structure of the surface layer [1] cannot be explained on the basis of a satellite absorption wave.

The effect of dissociation requires additional consideration, although on the basis of the above we may conclude that thermodissociation processes apparently do not play the dominant role in initiation, development, and motion of the absorption wave, at least in the case considered here, ZhS-12 glass. Since in the experiments clear signs of thermal decomposition of the medium were observed after laser action [1, 2], such as change in the index of refraction and coloration, it can be proposed that dissociation takes place behind the absorption front and the time for establishment of dissociation equilibrium is not less than the characteristic time of wave motion  $t_x = \chi/v^2 \sim 10^{-7}$  sec.

#### NOTATION

T, absolute temperature; q, laser radiation intensity; C, volume heat capacity of medium;  $\kappa(T)$ , thermal conductivity coefficient of medium; k(T), radiation absorption coefficient; L, length of focal region of focusing system; a, caustic spot radius;  $\chi$ , thermal diffusivity coefficient; h, Planck's constant; c, speed of light.

#### LITERATURE CITED

1. N. E. Kask, V. V. Radchenko, et al., "Optical discharge in glass," *Pis'ma Zh. Tekh. Fiz.*, 4, No. 13, 775-778 (1978).
2. N. V. Zelikin, N. E. Kask, et al., "Absorption wave observation in transparent dielectrics," *Pis'ma Zh. Tekh. Fiz.*, 4, No. 21, 1296-1300 (1978).
3. P. S. Kondratenko and B. I. Makshantsev, "Laser radiation absorption wave propagation in a solid transparent dielectric," *Zh. Eksp. Teor. Fiz.*, 66, No. 5, 1734-1739 (1974).
4. A. A. Kovalev and B. I. Makshantsev, "Role of radiationless transitions in light radiation absorption wave propagation in a solid transparent dielectric," *Fiz. Tverd. Tela*, 17, No. 1, 188-193 (1976).
5. M. I. Tribel'skii, "Steady-state motion of an opacity wave in optical breakdown of solid transparent media," *Fiz. Tverd. Tela*, 18, No. 5, 1347-1350 (1976).
6. I. E. Poyurovskaya, "Structure of the absorption wave in optical breakdown of transparent dielectrics," *Fiz. Tverd. Tela*, 19, No. 10, 2876-2878 (1977).
7. N. F. Mott and E. A. Davis, *Electronic Processes in Noncrystalline Materials*, Oxford Univ. Press (1971).
8. Y. P. Raizer, *Laser Induced Discharge Phenomena*, Plenum Publ. (1977).
9. M. N. Libenson, "Plasma-chemical model of optical breakdown of transparent dielectrics," *Pis'ma Zh. Tekh. Fiz.*, 3, No. 10, 446-450 (1977).
10. E. L. Klochan, S. P. Popov, and G. M. Fedorov, "Development of thermal instability in a transparent dielectric under the action of a quasicontinuous laser pulse," *Pis'ma Zh. Tekh. Fiz.*, 6, No. 8, 453-456 (1980).